*Journal of Sound and Vibration* (2002) **257**(4), 605–613
doi:10.1006/jsvi.5047, available online at http://www.idealibrary.com on IDEAL®

# FORCE FEEDBACK VERSUS ACCELERATION FEEDBACK IN ACTIVE VIBRATION ISOLATION

A. Preumont, A. François, F. Bossens and A. Abu-Hanieh

*Active Structures Laboratory, Université Libre de Bruxelles, CP* 165-42, 50 *Av. F.D. Roosevelt, B*-1050 *Brussels, Belgium. E-mail* : *andre.preumont@ulb.ac.be*

(*Received* 7 *August* 2001, *and in final form* 13 *December* 2001)

This paper compares the force feedback and acceleration feedback implementation of the sky-hook damper when it is used to isolate a flexible structure from a disturbance source. It is shown that the use of a force sensor produces always alternating poles and zeros in the open-loop transfer function between the force actuator and the force sensor, which guarantees the stability of the closed loop. On the contrary, the acceleration feedback produces alternating poles and zeros only when the flexible structure is stiff compared to the isolation system; this property is lost when the flexible modes of the sensitive payload interfere with the isolation system.



## 1. INTRODUCTION

Vibration isolation is concerned with the development of an interface between a vibration source and a vibration-sensitive equipment, which attenuates the vibration transmission above the corner frequency of the isolation system [1]. As an example, a precision payload (such as a telescope) must be isolated to be protected from the jitter induced by the reaction wheel assembly of the attitude control system of a spacecraft [2]. On the other hand, the isolation system must allow the low-frequency attitude control torque to be transmitted to the spacecraft.

Any passive isolation system consists of one or several stages of springs and dampers introduced in the vibration propagation path; their parameters are adjusted to achieve a desired corner frequency and a reasonable compromise between the amplification at the resonances and the high-frequency attenuation. The passive damping is necessary to limit the amplification at resonance, but it tends to reduce the high-frequency attenuation of the isolation system.

Active vibration isolation aims at improving the performance of the vibration isolation by including a force generating element in the isolation interface, a sensor at the receiving end of the transmission path, and a feedback control law connecting them. The celebrated *sky-hook* damper [3, 4] is a single-stage interface which allows one to combine a $-40$ dB/decade attenuation rate at high frequency with a critical damping (no overshoot) at resonance.

Section 2 reviews the sky-hook damper for the single degree-of-freedom (d.o.f.) isolator connecting two rigid bodies; it also discusses two sensing options (namely acceleration of the sensitive payload and the total force transmitted by the isolator). Next, the paper compares the two sensing options when the sensitive equipment is flexible, which is more representative of a large-space structure; in section 3 a two-d.o.f. sensitive equipment is

0022-460X/02/$35.00 

considered. In section 4, a general result is established, which guarantees the interlacing of the poles and zeros for a force feedback. Section 5 considers a free–free beam to illustrate the superiority of the force feedback option over the acceleration feedback when the flexible modes of the sensitive payload interfere with the isolation system.

## 2. SKY-HOOK DAMPER

Consider the single-axis isolator connecting two rigid bodies as in Figure 1 ($x_d$ and $m$ are the displacement and mass of the disturbance source, $x_c$ and $M$ are the displacement and mass of the sensitive equipment, $s$ is the Laplace variable, $g$ is the control gain, $X_c(s)$ is the Laplace transform of $x_c$, $sX_c$ is the Laplace transform of $\dot{x}_c$, etc.). The classical implementation of the sky-hook damper is that of Figure 1(a): an acceleration sensor is placed on the sensitive equipment, measuring its absolute acceleration $\ddot{x}_c$ (or $s^2X_c$); the sensor signal is passed through an integral controller $(-g/s)$ leading to a control force proportional to the absolute velocity of the sensitive equipment, $F_a = -gsX_c$. The name *sky-hook damper* comes from the fact that this force could conceptually be achieved with a passive damper connecting the sensitive equipment to a fixed point in space (the sky, Figure 1(b)). Since the force applied to a rigid body is proportional to its acceleration, the feedback based on the acceleration $\ddot{x}_c$ of the sensitive equipment can alternatively be based on the sensing of the total interface force, $F = Ms^2X_c$ (Figure 1(c)). The two control configurations are totally equivalent and they have the same open-loop transfer function:

$$G(s) = \frac{F(s)}{F_a(s)} = \frac{Ms^2X_c(s)}{F_a} = \frac{mMs^2}{(mMs^2 + k(M+m))}. \tag{1}$$

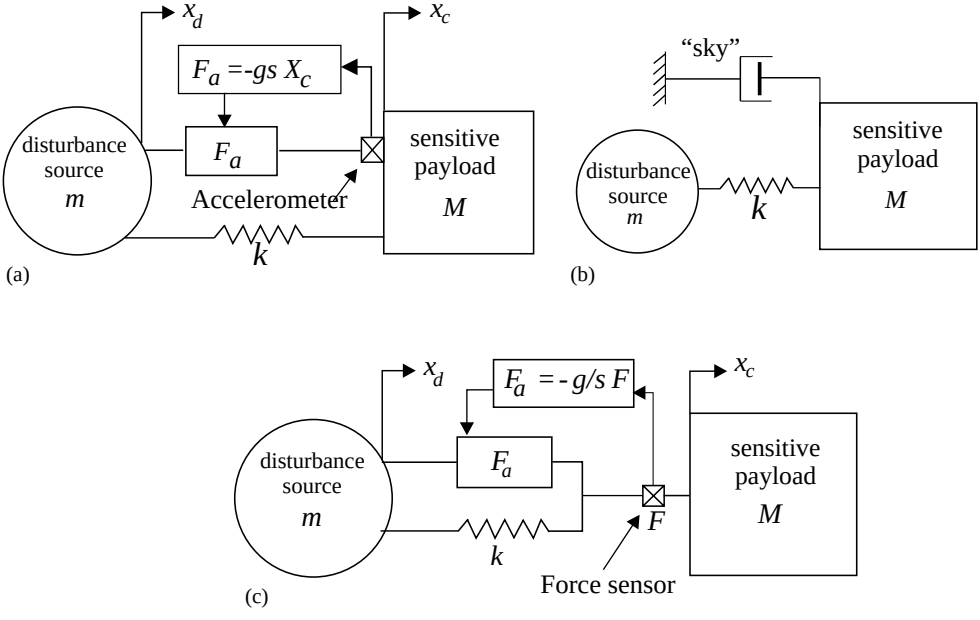


Figure 1. (a) Single-axis soft isolator with acceleration feedback, (b) equivalent "sky-hook" damper and (c) force feedback isolator.

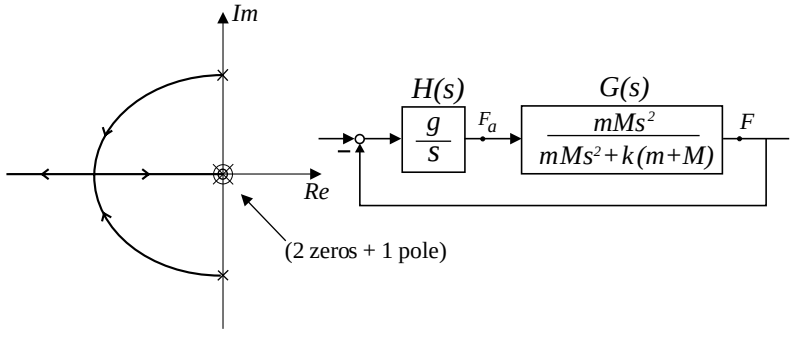


Figure 2. Root locus of the force feedback isolator connecting two rigid bodies.

With the compensator $H(s) = g/s$, the characteristic equation of the closed-loop poles reads

$$1 + gH(s)G(s) = 1 + g\frac{s}{(s^2 + \Omega^2)} = 0, \tag{2}$$

where $\Omega^2 = k(M+m)/mM$ is the natural frequency of the two-mass system; the corresponding root locus is represented in Figure 2. The transmissibility of the force feedback isolator reads

$$\frac{X_c(s)}{X_d(s)} = \left[\frac{M}{k}s^2 + \frac{M}{k}gs + 1\right]^{-1}, \tag{3}$$

which exhibits a $-40$ dB/decade attenuation rate at high frequency; the feedback gain $g$ can be adjusted to achieve critical damping at the corner frequency.

We now examine the deviation between the two control strategies when the payload is flexible.

## 3. FLEXIBLE PAYLOAD

Next, consider the situation where the sensitive payload is flexible as in Figure 3 (in the example of a spacecraft, the flexible appendage may represent a solar panel). The dynamics of the flexible payload is no longer governed by $F = ms^2X_c$, so that the two sensing options are no longer equivalent. In fact, different sensor configurations correspond to different locations of the open-loop transmission zeros in the complex plane. Before establishing a fairly general result on the stability of the force feedback, let us examine the simple example of Figure 3 with the following numerical values:

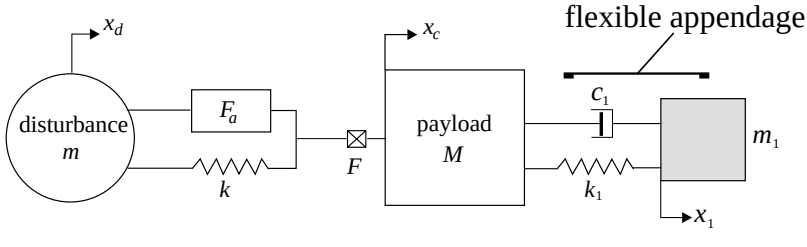


Figure 3. Payload with a flexible appendage.

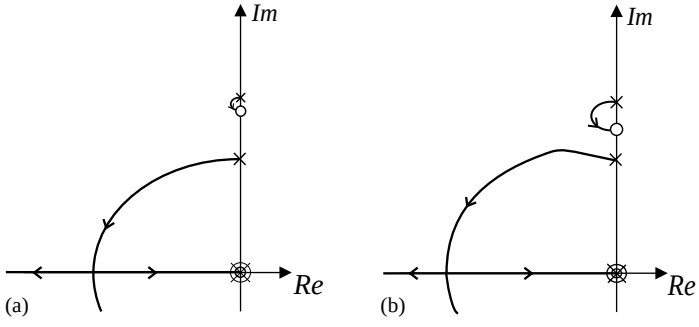


Figure 4. Root locus of the isolation system with a light flexible appendage ($m_1 = 0{\cdot}5$ kg). (a) Force feedback and (b) acceleration feedback, (only the upper half of the locus is shown).

$m = 1{\cdot}1$ kg, $M = 1{\cdot}7$ kg, $k = k_1 = 12\,000$ N/m, $c_1 = 0$ (assuming no damping, all the poles and zeros are on the imaginary axis); the mass $m_1$ of the flexible appendage is taken as a parameter to analyze the interaction between the flexibility of the payload and the isolation system. When $m_1$ is small, the frequencies of the additional pair of poles and zeros introduced by the flexible appendage are much higher than the isolator poles and the situation is not much different from that of a rigid body. As $m_1$ increases, they move along the imaginary axis towards the lower frequencies. Figure 4 shows the root locus plots for $m_1 = 0{\cdot}5$ kg; the acceleration feedback and the force feedback have similar root locus plots, with a new pole/zero pair appearing higher on the imaginary axis; the only difference between the two plots is the distance between the pole and the zero which is larger for the acceleration feedback; as a result, the acceleration feedback produces a larger damping of the higher mode. On the contrary, when $m_1$ is large, the root locus plots are reorganized as shown in Figure 5 for $m_1 = 3{\cdot}5$ kg. In the case of force feedback (Figure 5(a)), the poles and zeros still alternate on the imaginary axis, leading to a stable root locus; this property is lost for the acceleration feedback (Figure 5(b)), leading to an unstable loop for the lower mode. In practice, the presence of damping ($c_1 \neq 0$) moves this loop slightly to the left and allows to operate the control system for small gains, not enough, however to achieve critical damping on the suspension poles. Large space structures are usually very lightly damped. We now establish the central result of this paper.

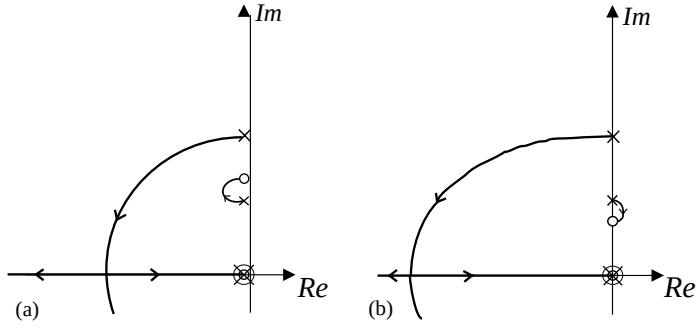


Figure 5. Root locus of the isolation system with a heavy flexible appendage ($m_1 = 3{\cdot}5$ kg): (a) Force feedback and (b) acceleration feedback.

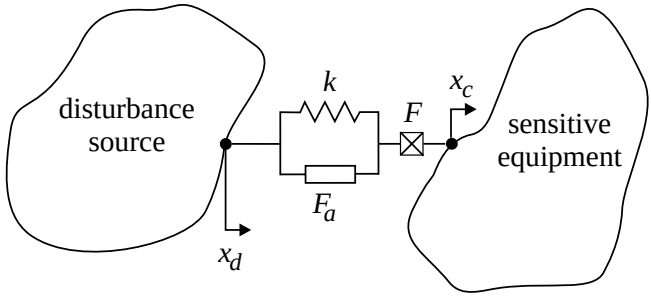


Figure 6. Two arbitrary flexible structures connected with a single-axis soft isolator with force feedback.

## 4. OPEN-LOOP POLE/ZERO PATTERN OF A SOFT ISOLATOR WITH FORCE FEEDBACK

The following result confirms the observation of the previous example.

If two arbitrary flexible, undamped structures are connected with a single-axis soft isolator with force feedback (Figure 6), the poles and zeros in the open-loop transfer function $F(s)/F_a(s)$ alternate on the imaginary axis.

The proof stems from the property of the collocated systems with *energetically conjugated* input and output variables (e.g., force input and displacement output, or torque input and angle output): For such a system, all the residues in the modal expansion of the transfer function have the same sign and this results in alternating poles and zeros on the imaginary axis [5, 6].

If we now examine the transfer function between the control force $F_a$ and the output of the force sensor $F$ (Figure 6), although the actuator and sensor are collocated, $F$ and $F_a$ are not energetically conjugated and the preceding property does not apply. However, the total force $F$ transmitted by the isolator is the sum of the control force $F_a$ and the spring force, $k\Delta x$, where $\Delta x$ is the relative displacement of the two structures along the isolator axis,

$$F = k\Delta x - F_a$$

or

$$\frac{F(s)}{F_a(s)} = k\frac{\Delta X(s)}{F_a(s)} - 1. \tag{4}$$

Thus, the open-loop transfer function $F/F_a$ is the sum of $k\Delta X/F_a$ and a negative unit feedthrough. The input $F_a$ and the output $\Delta x$ involved in the transfer function $\Delta X/F_a$ are energetically conjugated and, as a result, the transfer function $\Delta X/F_a$ has all its residues positive and possesses alternating poles and zeros along the imaginary axis. The addition of a feedthrough term does not affect the residues in the modal expansion; the frequency response function (FRF) $F(\omega)/F_a(\omega)$ (obtained from the transfer function by setting $s = j\omega$, and which is purely real if the system is undamped) is obtained from the FRF $\Delta X(\omega)/F_a(\omega)$ by moving it along the ordinate axis by the amount of feedthrough; this changes the location of the zeros, without however changing the interlacing property (Figure 7).

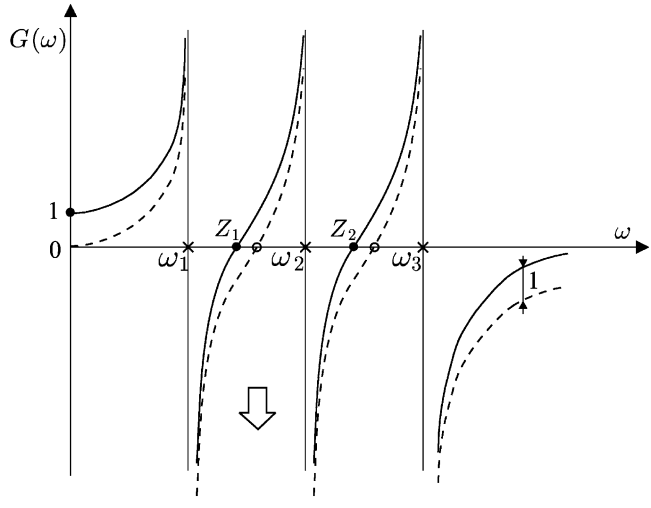


Figure 7. FRFs $k\Delta X(\omega)/F_a(\omega)$ and $F(\omega)/F_a(\omega)$ for an undamped structure (they are purely real). $\omega_i$ are the resonance frequencies and $Z_i$ the transmission zeros. The unit feedthrough component which appears in $F/F_a$ alters the location of the zeros (from ● to ○) without changing the interlacing property.

## 5. FREE–FREE BEAM

To illustrate further the influence of the sensing configuration on the pole/zero pattern, consider the free–free beam of Figure 8 with the following actuator/sensor configurations. This situation can be regarded as representative of a large space structure with its attitude control system (note that the rigid body modes are not controllable from the internal force $F_a$).

### 5.1. FREE--FREE BEAM ALONE

Consider the free–free beam of Figure 8(b) with a force actuator ($f$) and a collocated acceleration sensor ($\ddot{y}$); the poles are $\pm j\Omega_i$ where $\Omega_i$ are the natural frequencies of the free–free modes of the beam. According to the physical interpretation of the zeros [7], they represent the resonances of the subsystem constrained by the sensor and the actuator. In this case, the constrained subsystem has an additional support as on the right side of Figure 8(b); the zeros are $\pm jZ_i$ where $Z_i$ are the natural frequencies of the constrained system. Since the system is collocated and the input and output variables are energetically conjugated, the poles and zeros alternate on the imaginary axis:

$$Z_i < \Omega_i < Z_{i+1}. \tag{5}$$

### 5.2. COMPLETE SYSTEM WITH FORCE SENSOR

Next, consider the full system including the beam and the isolator with a force sensor (Figure 8(d)). The poles are $\pm j\omega_i$, where $\omega_i$ are the natural frequencies of the global system (beam + isolator) while the transmission zeros are obtained as the resonances of the constrained subsystem, where the interface force between the isolator and the beam is constrained to be zero; this is equivalent to releasing the isolator from the beam, which means that the zeros are $\pm j\Omega_i$ where $\Omega_i$ are the natural frequencies of the free–free beam (same as the poles for the configuration of Figure 8(b)). We know from the previous

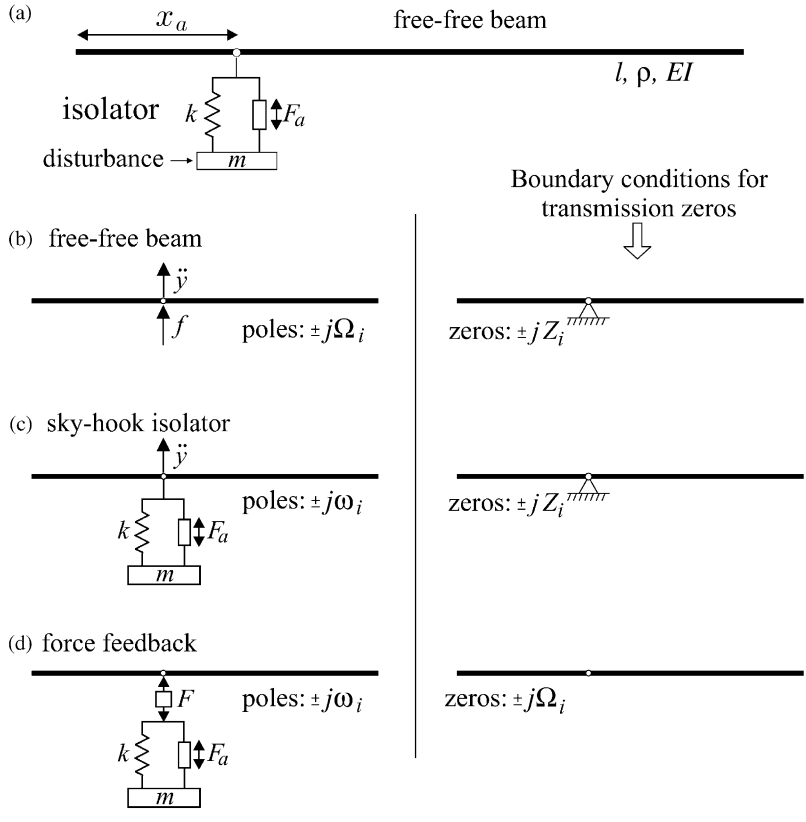


Figure 8. (a) Free–free beam and single-axis isolator. The other figures illustrate the various situations and the boundary conditions corresponding to the transmission zeros. (b) Free–free alone beam with displacement sensor and point force actuator. (c) Free–free beam and sky-hook isolator (acceleration sensor). (d) Free–free beam and isolator with force feedback.

section that the poles and the zeros also alternate in this configuration:

$$\omega_i < \Omega_i < \omega_{i+1}. \tag{6}$$

### 5.3. COMPLETE SYSTEM WITH ACCELERATION SENSOR

This is the configuration of Figure 8(c), where an acceleration sensor has been substituted to the force sensor. The poles $\pm j\omega_i$ are the same as in the previous case (the poles do not depend on the sensor configuration) and the transmission zeros, corresponding to the resonances of the constrained subsystem where the acceleration of the connecting d.o.f. is zero, are $\pm jZ_i$, identical to those of Figure 8(b). No guarantee exist as to the interlacing of the poles and zeros for this sensor configuration, and it is easy to generate an example where this property is violated.

To illustrate this, Figure 9 shows the result of a numerical study performed with the numerical values given in the figure. The bending stiffness $EI$ of the beam is taken as parameter. The figure shows the evolution of the poles ($\omega_i$) and zeros ($\Omega_i$ and $Z_i$) of the various configurations as the flexibility of the beam increases (the frequency is made non-dimensional by dividing by the constrained natural frequency of the isolator,

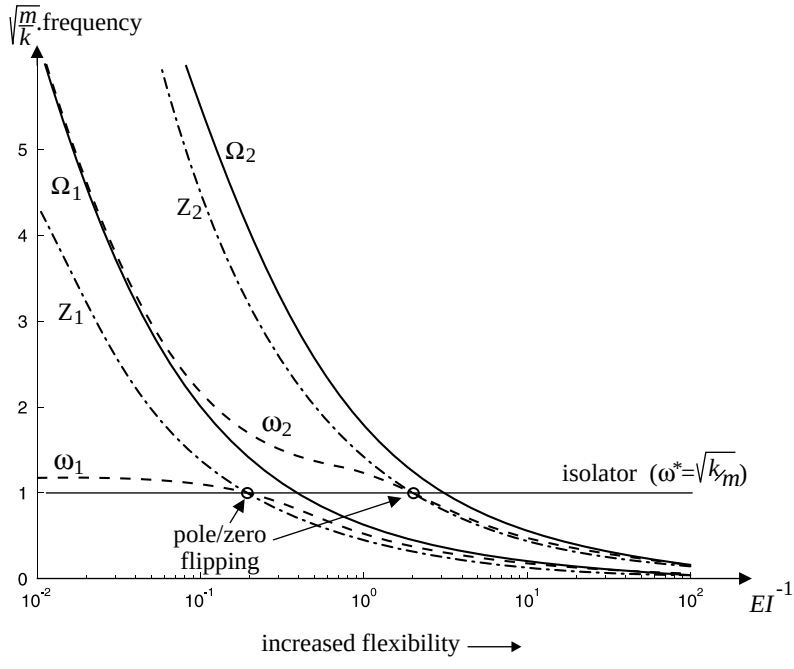


Figure 9. Flexible beam with an isolator; evolution of $\omega_i$, $Z_i$ and $\Omega_i$ with the flexibility of the beam.

$\omega^* = \sqrt{k/m}$). The MATLAB simulation uses a truncated modal expansion (3 flexible modes) with the analytical mode shapes of the free–free beam, including a quasi-static correction for the high-frequency modes (e.g. reference [6], chapter 2).

As expected, the two interlacing properties (5) and (6) are always satisfied. When the beam is stiff, the interlacing property $\omega_i < Z_i < \omega_{i+1}$ is satisfied and the stability of the sky-hook damper is therefore guaranteed, but as the beam becomes more flexible, the values of $\omega_i$ and $Z_i$ decrease at different rates and a pole/zero flipping occurs when they both become equal to the constrained frequency of the isolator, $\omega^*$. Beyond this point, the stability of the sky-hook damper is no longer guaranteed. This confirms the observations of the previous sections.

## 6. CONCLUSIONS

The sky-hook damper was originally developed with an acceleration measurement on the sensitive payload; an alternative implementation consists of measuring the total force transmitted across the isolator. The two strategies are totally equivalent in the case of a single-axis isolator connecting two rigid bodies.

When the isolator connects flexible bodies, acceleration and force measurements are no longer equivalent. It has been shown that the use of a force sensor always produces alternating poles and zeros in the open-loop transfer function; this guarantees the stability of the closed-loop system in all circumstances. On the contrary, acceleration feedback does not exhibit alternating poles and zeros any longer when the flexible modes of the sensitive payload interfere with the isolation system.

## ACKNOWLEDGMENTS

This work was supported by the Inter University Attraction Pole IUAP-IV-24 on Intelligent Mechatronics Systems.

## REFERENCES

1. C. Crede 1951 *Vibration and Shock Isolation*. New York: Wiley.
2. R. A. Laskin and S. W. Sirlin 1986 *American Institute of Aeronautics and Astronautics Journal of Guidance and Control* **9**, 469–477. Future payload isolation and pointing system technology.
3. D. C. Karnopp and A. K. Trikha 1969 *Transactions of American Society of Mechanical Engineers*, *Journal of Engineering for Industry*, *Series B* **91**, 1128–1132. Comparative study of optimization techniques for shock and vibration isolation.
4. C. E. Kaplow and J. R. Velman 1980 *American Institute of Aeronautics and Astronautics Journal of Guidance and Control* **3**, 227–233. Active local vibration isolation applied to a flexible space telescope.
5. G. D. Martin 1978 *Ph.D. Thesis*, *Stanford University*. On the control of flexible mechanical systems.
6. A. Preumont 1997 *Vibration Control of Active Structures*: *An Introduction*, 22–25. Dordrecht: Kluwer.
7. D. K. Miu 1993 *Mechatronics*. Berlin: Springer-Verlag; chapter 8.